J. Electrochem. Sci. Eng. **12(2)** (2022) 293-304; http://dx.doi.org/10.5599/jese.1162

Open Access : : ISSN 1847-9286

https://pub.iapchem.org/ojs/index.php/JESE

Original scientific paper

Synthesis and antioxidant activity of six novel N-ferrocenylmethyl-N-(nitrophenyl)- and -N-(cyanophenyl)-acetamides: Cyclic voltammetry and molecular docking studies

Abdellatif Kedadra, Touhami Lanez✉, Elhafnaoui Lanez, Hadia Hemmami and Meriem Henni

VTRS Laboratory, Department of Chemistry, Faculty of Sciences, University of El Oued B.P.789, 39000, El Oued, Algeria

Corresponding author: ✉*touhami-lanez@univ-eloued.dz;*

Received: November 8, 2021; Accepted: December 28, 2021; Published: January 25, 2022

Abstract

Cyclic voltammetry (CV) assays were performed to measure superoxide anion radical ($O^{\cdot}_2^-$) scavenging activities of six novel N-ferrocenylmethyl-N-(nitrophenyl)-acetamides and N-ferrocenylmethyl-N-(cyanophenyl)acetamides (FMA1-FMA6), followed by molecular docking simulations and in silico toxicity prediction. The obtained values of IC_{50} from CV assays indicated that all studied compounds showed promising scavenging activity against $O^{\cdot}_2^-$ radicals, with the compounds FMA1, FMA3, and FMA4 possessing the most significant potency. A molecular docking study revealed that all compounds interact with amino acid residues of glutathione reductase via hydrogen bonding and hydrophobic interactions. The compound FMA4 was the most inactive compound against the glutathione reductase enzyme having the highest inhibitory concentration of 2.61 µM and the lowest docking score of -31.85 kJ/mol. Toxicity studies demonstrated that among six studied compounds, FMA4, FMA5, and FMA6 are predicted to be nontoxic.

Keywords

Ferrocene derivatives; superoxide anion radical; binding free energy; toxicity study

Introduction

Recently, ferrocene derivatives have been widely studied because of their versatile potential applications in many research fields such as medicinal chemistry [1–7], material sciences [8], and diagnostic applications fields [9]. N-ferrocenylmethylamines and their derivatives, in particular, N-ferrocenylmethyl-N-(nitrophenyl)- and -N-(cyanophenyl)aniline, have shown important biological activities due to their promising biological potential as anticancer properties [10,11], antimicrobial agents [12], antioxidants [13,14], and anti-proliferative agents against MCF-7 human breast cancer cell lines [15].

Most of ferrocenylmethylaniline derivatives scavenge superoxide free radicals, and this reaction is useful in the inhibition of cancer growth [16]. The superoxide radical scavenging activities of ferrocenylmethylanilines are mainly due to the presence of functionalized aniline in the ferrocene moiety that could donate protons to the superoxide anion radical to form the corresponding radical species. The mechanism might be described by a first proton transfer (Eq. (1)), followed by the electron transfer (Eq. (2)). With a second proton transfer (Eq. (3)) the overall reaction is a two-electron reduction of oxygen (Eq. (4)). In our experimental conditions with ferrocene derivatives, we did not observe the increase of oxygen current reduction, which is expected in the hypothesis of a proton donating mechanism [17].

$$O^{\cdot}{}_2^- + FcH \rightarrow HO^{\cdot}{}_2 + Fc^- \quad (1)$$

$$HO^{\cdot}{}_2 + O^{\cdot}{}_2^- \rightarrow HO_2^- + O_2 \quad (2)$$

$$HO_2^- + FcH \rightarrow H_2O_2 + Fc^- \quad (3)$$

$$O^{\cdot}{}_2^- + 2e + FcH \rightarrow H_2O_2 + 2Fc^- \quad (4)$$

Glutathione, a tripeptide protein naturally produced by the body, is made up of three amino acids: glutamic acid, cysteine, and glycine. It plays an essential antioxidant intracellular role [18], since it is involved in the elimination of reactive oxygen species and acts as a scavenger for various oxygen radicals. The enzyme glutathione reductase (GR), also called glutathione-disulfide reductase, reduces the oxidized form of glutathione disulfide (GSSG) to the reduced glutathione form (GSH). Elevated levels of GSSG/GSH ratio lead to intracellular signal transduction, elimination of free radicals and reactive oxygen species, and the preservation of intracellular redox status [19]. Thus, inhibition of glutathione reductase results in a decrease in GSH, an increase in GSSG, and consequently a high GSSG/GSH ratio. Studying the glutathione reductase inhibition by potentially antioxidant compounds could serve for choosing antioxidants candidates. A good antioxidant candidate should inhibit glutathione reductase enzyme less.

In this work, we describe the synthesis and the scavenging activity against $O^{\cdot}{}_2^-$ of six novel N-ferrocenylmethyl-N-(nitrophenyl)- and N-ferrocenylmethyl-N-(cyanophenyl)acetamides using cyclic voltammetry assays. Further, the compounds were scrutinized through toxicity study and molecular docking to predict the median lethal dose (LD_{50}) and the toxicity class (TC) to afford an insight into the inhibition and binding partialities of the most potent compounds with glutathione reductase.

Experimental

Chemicals

All starting materials and solvents used for the synthesis of N-ferrocenylmethyl-N-(nitrophenyl)- and N-ferrocenylmethyl-N-(cyanophenyl)acetamides were of analytical grade and obtained from different commercial sources and used as received. Tetrabutylammonium tetra-fluoroborate (Bu_4NBF_4) (electrochemical grade 99 %) was from Sigma-Aldrich. Oxygen gas (research-grade 99.99 %) was supplied by Linde Gaz Algérie.

Materials and methods

CV experiments were run on a PGZ301 potentiostat (Radiometer Analytical SAS, France) connected to an electrochemical cell having a volume of 15 mL and equipped with three electrodes: a glassy carbon working electrode of an area equal to 0.013 cm^2, a platinum wire auxiliary electrode, and a Hg/Hg_2Cl_2 reference electrode. The reaction medium was saturated with high-purity commercial oxygen for 15 min before each experiment. ^1H NMR spectra were obtained on a Bruker

Avance DPX 300 MHz spectrometer. All ^{1}H NMR spectra are reported in ppm relative to the central line of the singlet for $CDCl_3$ at 7.28 ppm.

Structure optimization was run using density functional theory implemented in Gaussian 09 package [20]. All calculations were carried out with the unrestricted Becker's three-parameter hybrid exchange functional [20] combined with Lee-Yang-Parr nonlocal correlation function, abbreviated as B3LYP [22–24] with combined basic sets, LanL2DZ [25–27] for optimizing iron atom and 6-311G+(d) for the rest of atoms [28–30].

The in silico toxicity study was performed using the ProTox-II web server [31].

Molecular docking simulations were performed using AutoDock 4.2 docking software [32,33], executed on a Pentium 2.7 GHz and 8 GB Ram microcomputer MB memory with windows 8 operating system.

Synthesis

N-ferrocenylmethyl-N-(nitrophenyl)- and N-ferrocenylmethyl-N-(cyanophenyl)acetamides coded as FMA1-FMA6 were synthesized by coupling the well-known quaternary salt (ferrocenylmethyl)-trimethyl-ammonium iodide [34] with the corresponding substituted anilines, following our previously reported procedure [35,36]. The obtained products were then acetylated using acetic anhydride and their molecular structures are shown in Figure 1. The antioxidant activities of the synthesized compounds against superoxide anion radicals were measured using CV assays.

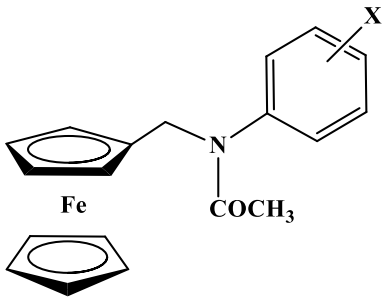

FMA1, X = 2-NO_2; FMA2, X = 3-NO_2; FMA3, X = 4-NO_2;
FMA4, X = 2-CN; FMA5, X = 3-CN; FMA6, X = 4-CN

Figure 1. *Chemical structures of N-ferrocenylmethyl-N-(nitrophenyl)-acetamide and N-ferrocenylmethyl-N-(cyanophenyl)acetamide*

General procedure for the synthesis of compounds (FMA1-FMA6)

The corresponding N-ferrocenylmethyl-N-(nitrophenyl)aniline (500 mg, 1.49 mmol) or N-ferrocenylmethyl-N-(cyanophenyl)aniline (500 mg, 1.58 mmol) was dissolved in acetic anhydride 160 ml (1.7 mmol) and the reaction mixture was heated at 65 °C for 30 minutes under an atmosphere of nitrogen. Then it was allowed to cool to room temperature and poured on 140 ml 0.1 M of an aqueous solution of sodium carbonate and extracted three times with dichloromethane. The combined extracts were evaporated and the obtained residue was recrystallized from a mixture of methanol/water (30/70) to yield a red/orange yellowish solid.

Results and discussion

Antioxidant activity assays against superoxide anion radicals

Superoxide anion radicals ($O^{\cdot}{}_2^-$) scavenging activity assays were used to measure the antioxidant activity of N-ferrocenylmethyl-N-(nitrophenyl)- and N-ferrocenylmethyl-N-(cyanophenyl)-acetamides. The $O^{\cdot}{}_2^-$ was electrochemically generated in situ by one-electron reduction of commercial molecular oxygen dissolved in DMF containing 0.1 M tetrabutylammonium tetra-fluoroborate (Bu_4NBF_4) as a supporting electrolyte. Increased concentrations of each studied compound were then added to the electrochemical cell containing a solution of the generated $O^{\cdot}{}_2^-$, and the cyclic voltammograms were recorded after each addition of the test compounds, in the potential window

from −0.0 to −1.6 V at the scan rate of 0.1 V s^{-1}. Obtained voltammograms of oxygen-saturated DMF containing 0.1 M of Bu_4NBF_4 in the absence and presence of gradually increasing concentrations of the compounds FMA1-FMA6 in the same solvent are shown in Figure 2.

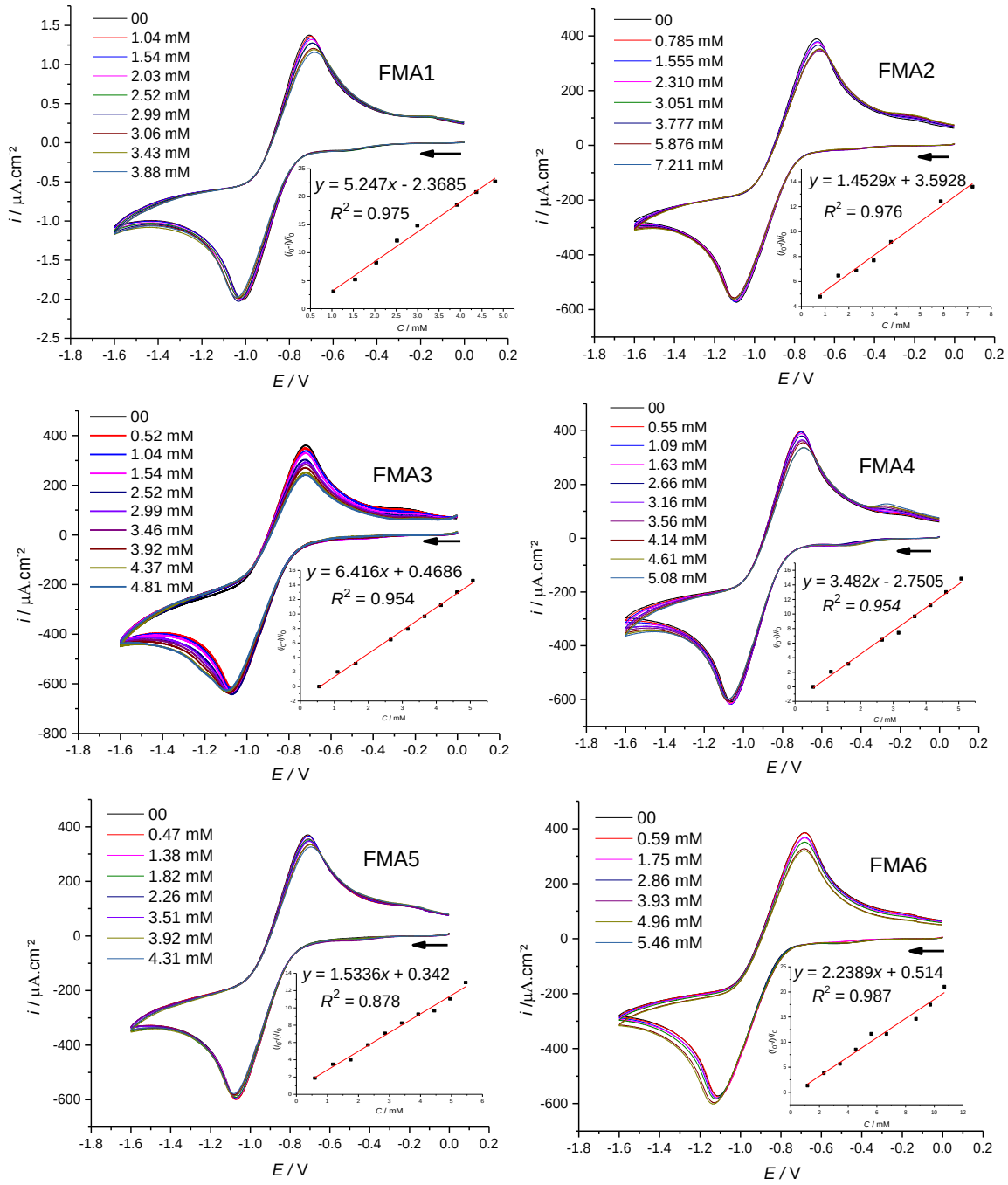

Figure 2. *Cyclic voltammograms of oxygen-saturated DMF in the absence and presence of gradually increased concentrations of FMA1-FMA6. Inset plots of [(i_0 – i) / i_0 vs. c]*

All voltammograms showed a decrease in the anodic peak current density of the $O^{\cdot}{}_2^-/O_2$ redox couple upon addition of gradually increasing concentration of test compounds, and this decrease was used for the calculation of the half-maximal inhibitory concentration (IC_{50}).

The inhibition of $O^{\cdot}{}_2^-$ was calculated using the following equation [17,37,38]

$$O^{\cdot}{}_2 \text{ scavenging activity} = \frac{i_0 - i}{i_0} 100 \quad (5)$$

where i_0 and i are the anodic peak current densities of the superoxide anion radical in the absence and presence of the test sample, respectively.

The half-maximal inhibitory concentration (IC_{50}) values were obtained from the plot of $O^{\bullet}{}_2^-$-scavenging activity against different compound concentrations (inset plots of Figure 2). The antioxidant activity has been expressed as IC_{50}. The IC_{50} value was defined as the concentration of the compound that inhibits the formation of $O^{\bullet}{}_2^-$ by 50 %.

Obtained values of IC_{50} shown in Figure 3 indicate that all N-ferrocenylmethyl-N-(nitrophenyl)- and N-ferrocenylmethyl-N-(cyanophenyl)acetamides showed promising scavenging activity against $O^{\bullet}{}_2^-$ radicals, with the activity of compounds FMA1, FMA3, and FMA4 almost comparable to that of the standard α-tocopherol (7.058 mM) used as a positive control.

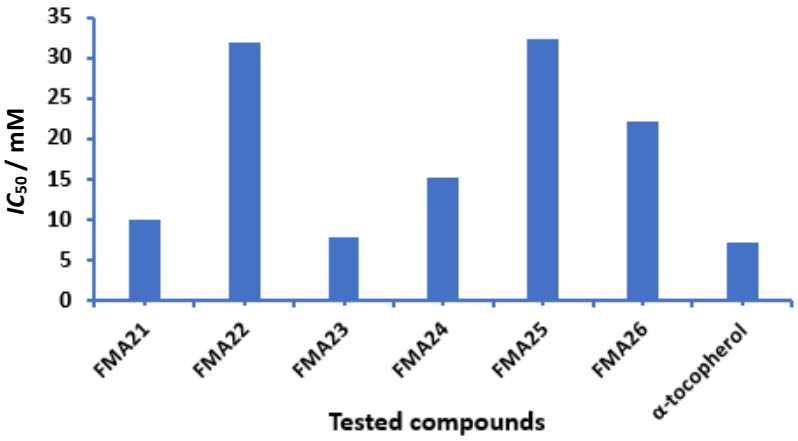

Figure 3. IC$_{50}$ *values of N-ferrocenylmethyl-N-(nitrophenyl)- and N-ferrocenylmethyl-N-(cyanophenyl)acetamides (FMA1-FMA6) and α-tocopherol as a positive control*

Molecular docking study

A molecular docking study was carried out to afford an insight into the inhibition and binding parameters of N-ferrocenylmethyl-N-(nitrophenyl)- and N-ferrocenylmethyl-N-(cyanophenyl)-acetamides with the enzyme glutathione reductase. The enzyme glutathione reductase (GR), also called glutathione-disulfide reductase, reduces glutathione disulfide (GSSG) to glutathione (GSH), which is involved in the elimination of reactive oxygen species and acts as a scavenger for various oxygen radicals. Glutathione exists in reduced (GSH) and oxidized (GSSG) forms, the reaction symbolized by the equation (6):

$$2GHS + NADP^+ \leftrightarrow GSSG + NADPH + H^+ \quad (6)$$

Inhibition of glutathione reductase results in a decrease in reduced glutathione (GSH) and an increase in glutathione disulfide (GSSG) using nicotinamide adenine dinucleotide phosphate (NADPH), particularly from the pentose phosphate pathway in bacteria, plants, and animals to regenerate glutathione, a molecule essential for resistance against oxidative stress and the preservation of intracellular pH. So, studying glutathione reductase inhibition could serve as a good means for the selection of antioxidants candidates. A good antioxidant candidate should reduce the inhibition of the glutathione reductase enzyme.

Rigid receptor and flexible ligand molecular docking models were carried out to study the inhibition of glutathione reductase by N-ferrocenylmethyl-N-(nitrophenyl)- and N-ferrocenylmethyl-N-(cyanophenyl)acetamides, and to understand how strong the interactions are between them. The crystal 3D structure of the glutathione reductase target involved in this study was retrieved from the online data bank, RCSB PDB (https://www.rcsb.org/pdb, ID: 1XAN) [40], Figure 4.

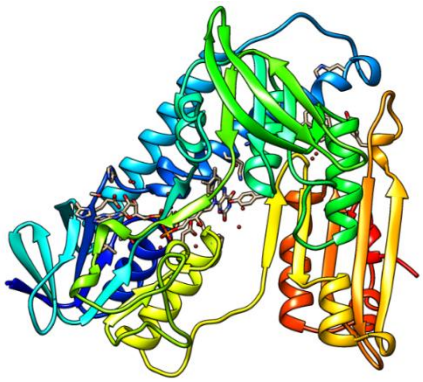

Figure 4. *UCSF chimera ribbons chemical structure view of human glutathione reductase in complex with a xanthene inhibitor (ID: 1xan)*

Receptor preparation

The receptor was first imported into the AutoDockTools interface. Missing atoms were inserted in incomplete residues, alternate conformations were deleted, all water molecules and ligands were removed, and polar hydrogen atoms and charges were added to the receptor structure.

Receptor-ligand docking

In silico molecular docking simulations studies were executed by using the AutoDock 4.2 software [32,33]. Lamarckian genetic algorithms were utilized with the grid box size set at 60×60×60 Å in the *x*, *y*, and *z* directions and the coordinates were fixed at *x* = 69.46, *y* = -17.32, and *z* = 55.62. All docking experiments consisted of 50 docking runs while the other parameters were left to their default values. The best conformation was selected with the lower docking energy for further docking analysis. The visualization of the interaction was generated with the PLIP webserver (protein-ligand interaction profiler) [41,42].

Results from the molecular docking suggest that hydrogen bonding, hydrophobic forces, and π-cation interactions are involved in the binding process. Figure 5 illustrates the interactions of compounds FMA1, FMA2, FMA3, FMA4, FMA5, and FMA6 with the nearby residues in the active site of glutathione reductase.

Interacting residues and their corresponding bond types and length are summarised in Table 1.

Table 1. *Interaction types between ligands FMA1, FMA2, FMA3, FMA4, FMA5, FMA6 and glutathione reductase*

Molecule	Bond type	Amino acid (number of bonds/interactions)	Distance, Å
FMA1	H-bonds	THR339 (2)	2.25, 2.00
	Hydrophobic interactions	ILE198(2), LEU338, PRO340, THR369, PHE372	3.89, 3.95, 3.27, 3.79, 3.41, 3.47
	π-Stacking interactions	TYR197	5.25
FMA2	H-bonds	THR339 (2)	2.62, 1.95
	Hydrophobic interactions	THR369(2), TYR197, ILE198, LEU338, PHE372	3.57, 3.55, 3.34, 3.62, 3.04, 3.45
FMA3	H-bonds	THR339	1.94
	Hydrophobic interactions	TYR197, LEU338, PRO340, THR369, PHE372	3.88, 3.21, 3.81, 3.41, 3.35
	π-stacking interactions	TYR197	5.42
FMA4	H-bonds	TYR197, THR339 (2)	3.10, 2.65, 2.01
	Hydrophobic interactions	THR57, TYR197, ILE198, LEU338, THR369, PHE372	3.82, 3.71, 3.85, 3.25, 3.47, 3.30
	π-stacking interactions	TYR197	5.25
FMA5	H-bonds	SER177, THR339 (2)	3.04, 3.29, 2.96
	Hydrophobic interactions	THR57, TYR197, ILE198, LEU338, THR369, PHE372	3.58, 3.49, 3.86, 3.10, 3.51, 3.37
FMA6	H-bonds	THR339 (2)	2.55, 1.93
	Hydrophobic interactions	THR57, TYR197, LEU338, THR369, PHE372	3.79, 3.56, 3.16, 3.44, 3.37

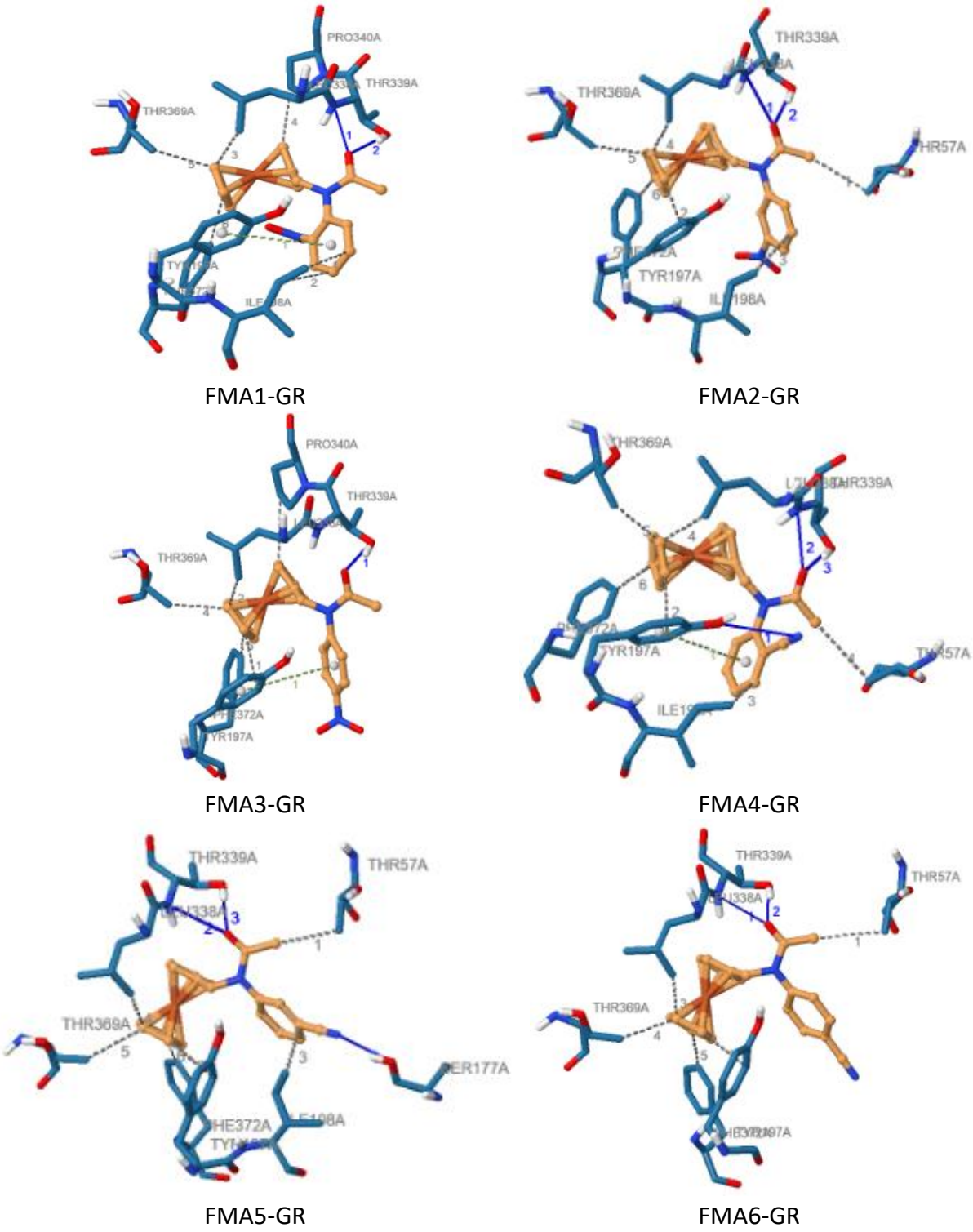

FMA1-GR FMA2-GR

FMA3-GR FMA4-GR

FMA5-GR FMA6-GR

Figure 5. *Best docking poses for glutathione reductase interacting with FMA1, FMA2, FMA3, FMA4, FMA5, and FMA6 illustrating H-bonds, hydrophobic, and π-cation interactions*

It can be seen from this table that besides hydrophobic interactions, compounds FMA4 and FMA5 formed with the GR three hydrogen bonds. Compounds FMA1, FMA2, and FMA6, however, reacted *via* two hydrogen bonds, while the compound FMA3 interacts only *via* one hydrogen bond beside one π-stacking interaction.

Obtained binding free energy and inhibitory concentration from molecular docking study for the compounds FMA1-FMA6 are summarised in Table 2.

Table 2. *Binding free energies and inhibitory concentration obtained from molecular docking study*

Adduct	FMA1-GR	FMA2-GR	FMA3-GR	FMA4-GR	FMA5-GR	FMA6-GR
ΔG / kJ mol^{-1}	-34.90	-34.82	-33.36	-31.85	-33.94	-33.56
IC_{50} / µM	0.76	0.79	1.42	2.61	1.11	1.31

In silico toxicity study

In silico toxicity study aims to help in optimizing compounds regarding their toxicity proprieties. The study could offer an important improvement to the awareness of the full perspective of virtual screening for the identification of target compounds with negligible or no toxicity, which may open a path for the selection of novel nontoxic ferrocenylmethylaniline derivatives with high antioxidant activity.

In silico toxicity study of the compounds FMA1-FMA6 was performed using the ProTox-II web server [31]. It aims to predict hepatotoxicity (Dili), carcinogenicity (Carcino), immunotoxicity (Immuno), mutagenicity (Mutagen), cytotoxicity (Cyto), median lethal dose (LD_{50}), and toxicity class (TC). According to in silico toxicity profiles presented in Table 3, the toxicity class of all compounds was detected to be equal to 3. FMA4, FMA5, and FMA6 were predicted to be nontoxic. FMA1, FMA2, and FMA3 were predicted to be toxic in mutagenicity.

Table 3. *In silico toxicity profiles of the studied compounds*

Molecule	Dili	Carcino	Immuno	Mutagen	Cyto	LD_{50} / mg kg^{-1}	TC
FMA1	inactive	active	inactive	active	inactive	237	3
FMA2	inactive	active	inactive	active	inactive	237	3
FMA3	inactive	active	inactive	active	inactive	237	3
FMA4	inactive	inactive	inactive	inactive	inactive	256	3
FMA5	inactive	inactive	inactive	inactive	inactive	237	3
FMA6	inactive	inactive	inactive	inactive	inactive	256	3

Based on the obtained results from the antioxidant study, molecular docking simulations and toxicity prediction, the compounds FMA2, FMA5, and FMA6 cannot be accepted as antioxidant candidates because they have the lowest antioxidant activity (Figure 1), the highest binding affinities, and the highest inhibitory activities towards the enzyme glutathione reductase (Table 2). Furthermore, the compound FMA1 possesses the highest antioxidant activity (Figure 1), but it cannot be the best antioxidant candidate because it has the highest binding affinity towards the enzyme glutathione reductase and also possesses the lowest inhibitory concentration of 0.76 µM that is necessary to reduce the rate of glutathione reductase enzyme reaction by 50 %. The compounds FMA4 and FMA3 possess the highest antioxidant activities, the lowest binding free energy of -31.85 and -33.36 kJ/mol, and the highest inhibitory concentration of 2.61 and 1.42 µM against glutathione reductase enzyme reaction, respectively, these values indicate weak binding affinity towards the enzyme glutathione reductase compared to the other compounds. Thus, the compounds FMA4 and FMA3 are weaker inhibitors of glutathione reductase. However, although compound FMA3 has higher antioxidant activity than FMA4, it cannot be a good antioxidant candidate because it is predicted as mutagenic (Table 3). Finally, based on what is cited above, the compound FMA4 can be chosen as the best antioxidant candidate.

Detailed procedure for the synthesis of compounds (FMA1-FMA6)

N- ferrocenylmethyl-N-(2-nitrophenyl)acetamide (FMA1)

N- ferrocenylmethyl-N-(2-nitrophenyl)acetamide (275 mg, 49 %) was obtained, as described above, m.p. 148 °C, orange solid.

IR (KBr:) ν = 3381 cm^{-1} (C-H), 1658 cm^{-1} (C=O), 1610 cm^{-1} (C=C), 1506 and 1572 cm^{-1} (C-NO_2)

UV-Vis: λ_{max} (CH_3CN) = 230 and 278 nm (π→π*, Fc, Ar), 431 nm (n→π*, NO_2, CO),

CV (ν = 100 mV s^{-1}, CH_3CN): i_{pa} = 26.02 µA cm^{-2}, i_{pc} = -25.09 µA cm^{-2}, i_{pa}/ i_{pc} = 1.04, E_{pa} = 508 mV *vs.* SCE, E_{pc} = 445 mV *vs.* SCE, ΔE = 63 mV, $E_{1/2}$ = 476.5 mV *vs.* SCE,

NMR ^{1}H (300 MHz, $CDCl_3$): δ = 1.91 ppm (3H, s, H1), 4.16 ppm (2H, m, H2), 4.23 ppm (2H, m, H3), 4.30 ppm (5H, s, H4), 4.64 ppm (2H, s, H5); 6.70 ppm (1H, dd, J = 11.03 Hz, H9), 6.92 ppm (1H, d, J = 11.37 Hz, H8), 7.49 ppm (1H, m, J = 22.18 Hz, H7), 8.24 ppm (1H, dd, J = 13.49 Hz, H6).

N- ferrocenylmethyl-N-(3-nitrophenyl)acetamide (FMA2)

N- ferrocenylmethyl-N-(3-nitrophenyl)acetamide (478 mg, 85 %) was obtained, as described above, m.p. 132 °C, orange leaflet.

IR (KBr:) ν = 3058 cm^{-1} (C-H), 1656 cm^{-1} (C=O), 1612 cm^{-1} (C=C) 1350 and 1531 cm^{-1} (C-NO_2),

UV-Vis: λ_{max} (CH_3CN)) = 232 and 325 nm (π→π*, Fc, Ar), 423 nm (n→π*, NO_2, CO),

CV (100 mV s^{-1}, CH_3CN): i_{pa} =8.06 µA cm^{-2}, i_{pc} = -8.18 µA cm^{-2}, i_{pa}/ i_{pc} = 0.98, E_{pa} = 534 mV *vs.* SCE, E_{pc} = 468 mV *vs.* SCE, ΔE = 66 mV, $E_{1/2}$ = 501 mV *vs.* SCE,

NMR ^{1}H (300 MHz, $CDCl_3$): δ = 1.87 ppm (3H, s, H1), 4.00 ppm (2H, m, H2), 4.07 ppm (2H, m, H3), 4.10 ppm (5H, s, H4), 4.67 ppm (2H, s, H5), 7.29 ppm (1H, t, J = 6.28Hz, H6), 7.53 ppm (1H, t, J = 8.94 Hz, H7), 7.90 ppm (1H, s, H9), 8.18 ppm (1H, d, J = 7.76 Hz H8).

N- ferrocenylmethyl-N-(4-nitrophenyl)acetamide (FMA3)

N- ferrocenylmethyl-N-(4-nitrophenyl)acetamide (461 mg, 82 %) was obtained, as described above, m.p. 158°C, red needles.

IR (KBr:) ν = 3075 cm^{-1} (C-H), 1659 cm^{-1} (C=O), 1602 cm^{-1} (C=C), 1593 cm^{-1} (C-NO_2),

UV-Vis: λ_{max} (CH_3CN)) = 232 nm (π→π*, Fc, Ar), λ = 380 nm (n→π*, NO_2, CO),

CV (100 mV s^{-1}, CH_3CN): i_{pa} = 9.62 µA cm^{-2}, i_{pc} = -9.73 µA cm^{-2}, i_{pa}/ i_{pc} = 0.99, E_{pa} = 494 mV *vs.* SCE, E_{pc} = 431 mV *vs.* SCE, ΔE = 63 mV, $E_{1/2}$ = 462.5 mV *vs.* SCE,

NMR ^{1}H (300 MHz, $CDCl_3$): δ = 1.87 ppm (3H, s, H1), 4.01 ppm (2H, m, H2), 4.07 ppm (2H, m, H3), 4.12 ppm (5H, s, H4), 4.69 ppm (2H, s, H5), 7.17 ppm (2H, d, J = 8.92Hz, H6), 8.22 ppm (2H, d, J = 8.94Hz, H7).

N-ferrocenylmethyl-N-(2-cyanophenyl)acetamide (FMA4)

N-ferrocenylmethyl-N-(2-cyanophenyl)acetamide (FMA4) (311 mg, 55 %) was obtained, as described above, m.p. 146°C, orange reddish solid.

IR (KBr:) ν = 3304 cm^{-1} and 3081 cm^{-1} (C-H), 2210.6 cm^{-1} (CN), 1602.3 cm^{-1} (C=O),

UV-Vis: λ_{max} (CH_3CN)) = 337 nm (π→π*, Fc, Ar), λ = 444 nm (n→π*, CO),

CV (100 mV s^{-1}, CH_3CN): i_{pa} = 100.61 µA cm^{-2}, i_{pc} = -102.13, i_{pa}/ i_{pc} = 1.015, E_{pa} = 525 mV *vs.* SCE, E_{pc} = 421 mV *vs.* SCE, ΔE = 99 mV, $E_{1/2}$ = 475 mV *vs.* SCE,

NMR ^{1}H (300 MHz, $CDCl_3$): δ = 2.13 ppm (3H, s, H1), 4.02 ppm (2H, m, H2), 4.20 ppm (2H, m, H3), 4.22 ppm (5H, s, H4), 4.26 ppm (2H, s, H5), 7.12-7.19 ppm (3H, m, J = 8.92Hz, H7,H8,H9), 7.55 ppm (2H, d, J = 18.95Hz, H6).

N-ferrocenylmethyl-N-(3-cyanophenyl)acetamide (FMA5)

N-ferrocenylmethyl-N-(3-cyanophenyl)acetamide (FMA4) (345 mg, 61 %) was obtained, as described above, m.p. 162°C, orange reddish solid.

IR (KBr:) ν = 3081 cm^{-1} (C-H), 2214.2 cm^{-1} (CN), 1636.1 cm^{-1} (C=O),

UV-Vis: λ_{max} (CH_3CN)) = 433.5 nm (n→π*, CO),

CV (100 mV s^{-1}, CH_3CN): i_{pa} = 10.71, µA cm^{-2}, i_{pc} = -11.09 µA cm^{-2}, i_{pa}/ i_{pc} = 1.03, E_{pa} = 598 mV *vs.* SCE, E_{pc} = 463 mV *vs.* SCE, ΔE = 99 mV, $E_{1/2}$ = 531 mV *vs.* SCE,

NMR ^{1}H (300 MHz, $CDCl_3$): δ = 1.77 ppm (3H, s, H1), 3.99 ppm (2H, m, H2), 4.07 ppm (2H, m, H3), 4.10 ppm (5H, s, H4), 4.63 ppm (2H, s, H5),7.21 ppm (1H, d, J = 7.74Hz, H6), 7.29 ppm (1H, s, H7), 7.48 ppm (1H, t, J = 7.75Hz, H9), 7.61 ppm (1H, d, J = 7.74 Hz, H8).

N-ferrocenylmethyl-N-(4-cyanophenyl)acetamide (FMA6)

N-ferrocenylmethyl-N-(4-cyanophenyl)acetamide (FMA4) (385 mg, 68 %) was obtained, as described above, m.p. 155°C, yellow solid.

IR (KBr:) v = 3081 cm^{-1} (C-H), 2214.2 cm^{-1} (CN), 1636.1 cm^{-1} (C=O),

UV-Vis: λ_{max} (CH_3CN)) = 265.5 nm (π→π*, Fc, Ar),

CV (100 mV s^{-1}, CH_3CN): i_{pa} = 18.61, µA cm^{-2}, i_{pc} = - 18.76 µA cm^{-2}, i_{pa}/ i_{pc} =1, E_{pa} = 488 mV *vs.* SCE, E_{pc} = 426 mV *vs.* SCE, ΔE = 62 mV, $E_{1/2}$ = 457 mV *vs.* SCE,

NMR ^{1}H (300 MHz, $CDCl_3$): δ = 1.82 ppm (3H, s, H1), 4.01 ppm (2H, s, H2), 4.08 ppm (2H, m, H3), 4.12 ppm (5H, s, H4), 4.66 ppm (2H, s, H5), 7.13 ppm (2H, d, J = 8.39 Hz, H6),7.67 ppm (2H, d, J = 8.36 Hz, H7).

The ^{1}H NMR spectra of all the synthesized compounds presented in Figure 6 reveal one downfield singlet at δ= 1.77-2.13 ppm which is ascribed to methyl protons.

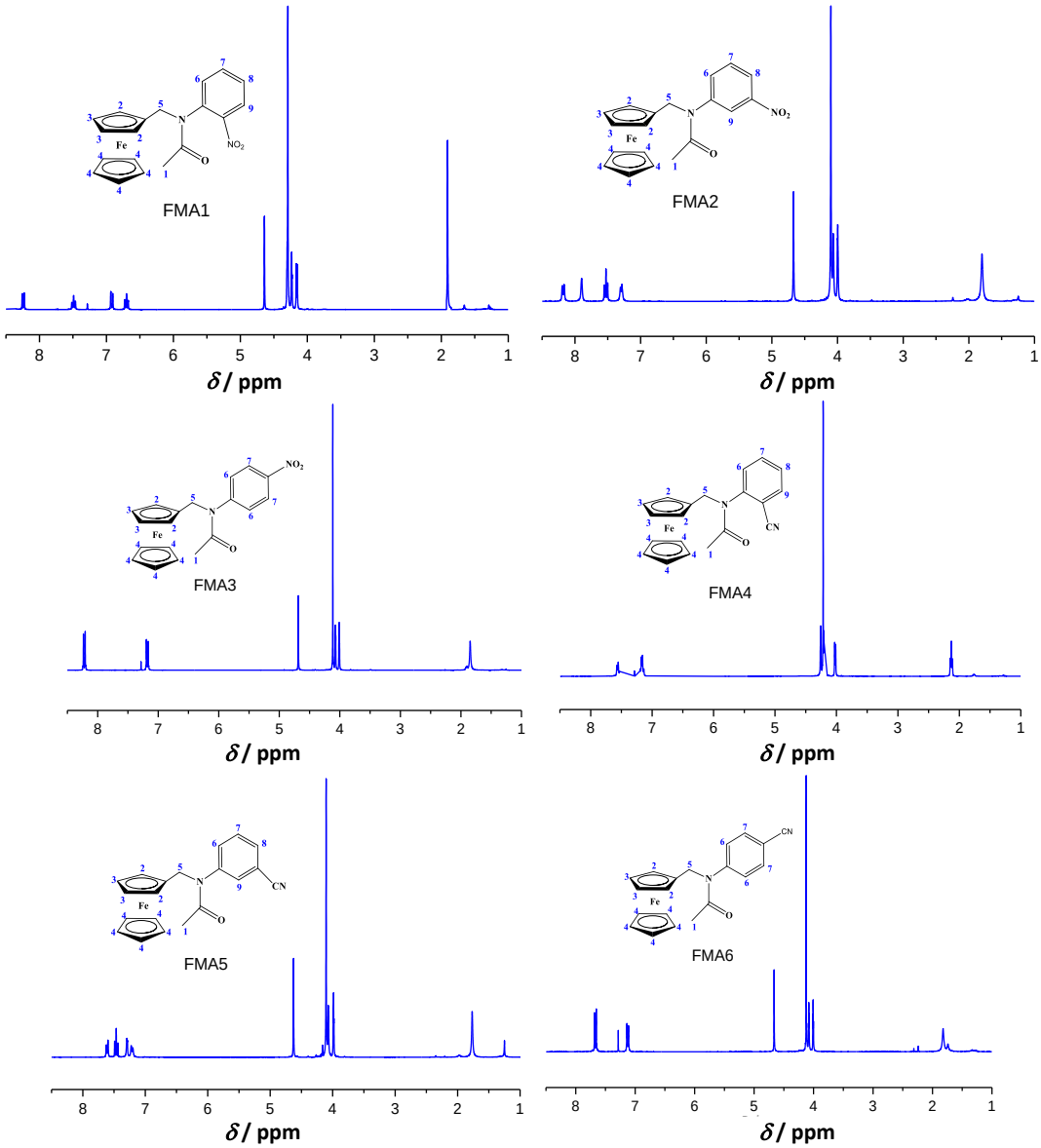

Figure 6. *^{1}H NMR spectra of FMA1, FMA2, FMA3, FMA4, FMA5, and FMA6 compounds*

The α- and β-protons of the substituted ring of ferrocene C_5H_4 appeared as a multiplet at 3.99-4.16 and 4.07-4.23 ppm respectively, the unsubstituted protons of the C_5H_5 ring of ferrocene appeared as a singlet at 4.10 to 4.30 ppm. A singlet appeared at δ = 4.26-4.69 ppm was due to methylene protons, this downfield shift of the methylene protons was observed due to electro-negativity of the nitrogen atom. The aromatic protons appeared in the range of δ= 6.70-8.24 ppm.

Conclusions

In this work, in vitro and in silico studies have been carried out to evaluate the scavenging activity against $O^{\cdot}_{2}{}^{-}$ and the antioxidant activity of six novel N-ferrocenylmethyl-N-(nitrophenyl)acetamides and N-ferrocenylmethyl-N-(cyanophenyl)acetamide using cyclic voltammetry assays. The obtained values of IC_{50} indicated that all derivatives showed promising scavenging activity against $O^{\cdot}_{2}{}^{-}$, with the compounds FMA1, FMA3, and FMA4 possessing the most significant potency. A molecular docking study and an *in silico* toxicity prediction revealed that compound FMA4 is the most inactive compound against glutathione reductase enzyme, having an inhibitory concentration of 2.61 µM and a docking score of -31.85 kJ mol^{-1}, which make the best good antioxidant candidate. The obtained in vitro and in silico results correspond with one another and give room for the design of novel antioxidant ferrocenylmethylaniline derivatives with less activity against glutathione reductase. The *in silico* toxicity study allowed us to predict the toxicity, the median lethal dose (LD_{50}), and the toxicity class (TC) of the studied compounds.

Acknowledgement: *The authors extend thanks and gratitude to the Directorate-general of scientific research and technological development (DGRSDT) of the Algerian Ministry of Higher Education and Research for financial support (project number B00L01UN390120150001).*

References

[1] X. Nie, Y. Xie, Q. Wang, H. Wei, C. Xie, Y. Li, B. Wang, Y. Li, *CyTA-Journal of Food* **19** (2021) 560-570. https://doi.org/10.1080/19476337.2021.1925746

[2] H. Chen, M. Chen, X. Wang, R. Sun, *Polymer Chemistry* **5** (2014) 4251-4258. https://doi.org-/10.1039/C4PY00120F

[3] Q. Zhou, M. Lei, Y. Wu, S. Li, Y. Tong, Z. Li, M. Liu, L. Guo, C. Chen, *Chemosphere* **279** (2021) 130584. https://doi.org/10.1016/j.chemosphere.2021.130584

[4] H. Mahmoudi-Moghaddam, S. Tajik, H. Beitollahi, *Food Chemistry* **286** (2019) 191-196. https://doi.org/10.1016/j.foodchem.2019.01.143

[5] X. Ma, M. Chao, Z. Wang, *Food Chemistry* **138** (2013) 739-744. https://doi.org/10.1016/-j.foodchem.2012.11.004

[6] E. Ertaş, H. Özer, C. Alasalvar, *Food Chemistry* **105** (2007) 756-760. https://doi.org/10.1016/-j.foodchem.2007.01.010

[7] M.I. López, I. Ruisánchez, M.P. Callao, *Spectrochimica Acta Part A: Molecular and Biomolecular Spectroscopy* **111** (2013) 237-241. https://doi.org/10.1016/j.saa.2013.04.031

[8] S. Anmei, Z. Qingmei, C. Yuye, W. Yilin, *Analytica Chimica Acta* **1023** (2018) 115-120. https://doi.org/10.1016/j.aca.2018.03.024

[9] D. Han, M. Yu, D. Knopp, R. Niessner, M. Wu, A. Deng, *Journal of Agricultural and Food Chemistry* **55** (2007) 6424-6430. https://doi.org/10.1021/jf071005j

[10] E. Mejia, Y. Ding, M.F. Mora, C.D. Garcia, *Food Chemistry* **102** (2007) 1027-1033. https://doi.org/10.1016/j.foodchem.2006.06.038

[11] X. Li, X. Sun, M. Li, *ChemistrySelect* **5** (2020) 12777-12784. https://doi.org/10.1002/slct.-202003559

[12] M. Heydari, S.M. Ghoreishi, A. Khoobi, *Measurement* **142** (2019) 105-112. https://doi.org/-10.1016/j.measurement.2019.04.058

[13] R. N. Adams, *Analytical Chemistry* **30** (1958) 1576–1579.

[14] B. J. Sanghavi, A. K. Srivastava, *Electrochimica Acta* **55** (2010) 8638–8648. https://doi.org/-10.1016/j.electacta.2010.07.093

[15] I. G. Svegl, B. Ogorevc, *Journal of Analytical Chemistry* **367** (2000) 701–706. https://doi.org/-10.1007/s002160000465

[16] G. Jeevanandham, K. Vediappan, Z. A. Alothman, T. Altalhi, A. K. Sundramoorthy, *Scientific Reports* **11** (2021) 13266. https://doi.org/10.1038/s41598-021-92620-2
[17] M. R. Ganjali, F. Garkani-Nejad, S. Tajik, H. Beitollahi, E. Pourbasheer, B. Larijanii, *International Journal of Electrochemical Science* **12** (2017) 9972-9982. https://doi.org-/10.20964/2017.11.49
[18] Y. Yao, X. Han, X. Yang, J. Zhao, C. Chai, *Chinese Journal of Chemistry* **39** (2021) 330-336. https://doi.org/10.1002/cjoc.202000398
[19] J. K. Patra, K. H. Baek, *Journal of Photochemistry and Photobiology B: Biology* **173** (2017) 291–300. https://doi.org/10.1016/j.jphotobiol.2017.05.045
[20] Y. Xie, T. Zhang, Y. Chen, Y. Wang, L. Wang, *Talanta* 2020, **213** (2020) 120843. https://doi.org/10.1016/j.talanta.2020.120843
[21] B. Sriram, M. Govindasamy, S. F. Wang, R. J. Ramalingam, H. Al-Lohedan, T. Maiyalagan, *Ultrasonics Sonochemistry* **58** (2019) 104618. https://doi.org/10.1016/j.ultsonch.2019.-104618
[22] H. Li, B. Kou, Y. Yuan, Y. Chai, R. Yuan, *Biosensors and Bioelectronics* **197** (2022) 113758. https://doi.org/10.1016/j.bios.2021.113758
[23] K.S. Park, Z. Ni, A.P. Côté, *Proceedings of the National Academy of Sciences* **103** (2006) 10186-10191. https://doi.org/10.1073/pnas.0602439103
[24] S.R. Venna, M.A. Carreon, *Journal of the American Chemical Society* **132** (2009) 76-78. https://doi.org/10.1021/ja909263x
[25] C. Chizallet, S. Lazare, D. Bazer-Bachi, F. Bonnier, V. Lecocq, E. Soyer, A. A. Quoineaud, N. Bats, *Journal of the American Chemical Society* **132** (2010) 12365-12377. https://doi.org/-10.1021/ja907359t
[26] H. Bux, F. Liang, Y. Li, J. Cravillon, M. Wiebcke, J. Caro, *Journal of the American Chemical Society* 131 (2009) 16000-16001. https://doi.org/10.1021/ja907359t
[27] S. L. Li, Q. Xu, *Energy & Environmental Science* **6** (2013) 1656-1683. https://doi.org/-10.1039/C3EE40507A
[28] M. C. Buzzeo, R. G. Evans, R. G. Compton, *ChemPhysChem* **5** (2004) 1106-1120. https://doi.org/10.1002/cphc.200301017
[29] A. Abo-Hamad, M. A. Alsaadi, M. Hayyan, I. Juneidi, M. A. Hashim, *Electrochimica Acta* **193** (2016) 321-343. https://doi.org/10.1016/j.electacta.2016.02.044
[30] M. Shahsavari, S. Tajik, I. Sheikhshoaie, H. Beitollahi, *Topics in Catalysis* (2021). https://doi.org/10.1007/s11244-021-01471-8
[31] A. J. Bard, L. R. Faulkner, *Electrochemical Methods; Fundamentals and Applications,* 2nd Edition, Wiley, 2001, pp. 580-632. ISBN 978-0-471-04372-0
[32] E. Prabakaran, K. Pandian, *Food Chemistry* **166** (2015) 198-205. https://doi.org/10.1016/j.-foodchem.2014.05.143
[33] Q. Ye, X. Chen, J. Yang, D. Wu, J. Ma, Y. Kong, *Food Chemistry* **287** (2019) 375-381. https://doi.org/10.1016/j.foodchem.2019.02.108
[34] Z. Mo, Y. Zhang, F. Zhao, F. Xiao, G. Guo, B. Zeng, *Food Chemistry* **121** (2010) 233-237. https://doi.org/10.1016/j.foodchem.2009.11.077
[35] V. Vinothkumar, A. Sangili, S. M. Chen, T. W. Chen, M. Abinaya, V. Sethupathi, *International Journal of Electrochemical Science* **15** (2020) 2414-2429. https://doi.org/10.20964/2020.03.08